Cite as: P. L. McMahon *et al.*, *Science* 10.1126/science.aah5178 (2016).

# A fully-programmable 100-spin coherent Ising machine with all-to-all connections

**Peter L. McMahon,[1,2*†] Alireza Marandi,[1*†] Yoshitaka Haribara,[2,3,4] Ryan Hamerly,[1] Carsten Langrock,[1] Shuhei Tamate,[2] Takahiro Inagaki,[5] Hiroki Takesue,[5] Shoko Utsunomiya,[2] Kazuyuki Aihara,[3,4] Robert L. Byer,[1] M. M. Fejer,[1] Hideo Mabuchi,[1] Yoshihisa Yamamoto[1,6]**

[1]E. L. Ginzton Laboratory, Stanford University, Stanford, CA 94305, USA. [2]National Institute of Informatics, 2-1-2 Hitotsubashi, Chiyoda-ku, Tokyo 101-8430, Japan. [3]Department of Mathematical Informatics, University of Tokyo, 7-3-1 Hongo, Bunkyo-ku, Tokyo 113-8656, Japan. [4]Institute of Industrial Science, The University of Tokyo, 4-6-1 Komaba, Meguro-ku, Tokyo 153-8505, Japan. [5]NTT Basic Research Laboratories, 3-1 Morinosato, Wakamiya, Atsugi, Kanagawa 243-0198, Japan. [6]ImPACT Program, Japan Science and Technology Agency, Gobancho 7, Chiyoda-ku, Tokyo 102-0076, Japan.

†These authors contributed equally to this work.

*Corresponding author. E-mail: pmcmahon@stanford.edu (P.L.M.); marandi@stanford.edu (A.M.)

**Unconventional, special-purpose machines may aid in accelerating the solution of some of the hardest problems in computing, such as large-scale combinatorial optimizations, by exploiting different operating mechanisms than standard digital computers. We present a scalable optical processor with electronic feedback that can be realized at large scale with room-temperature technology. Our prototype machine is able to find exact solutions of, or to sample good approximate solutions to, a variety of hard instances of Ising problems with up to 100 spins and 10,000 spin-spin connections.**

Combinatorial optimization problems, including many NP-hard problems, are central in numerous important application areas, including operations and scheduling, drug discovery, finance, circuit design, sensing, and manufacturing. Despite large advances in both algorithms and digital computer technology, even typical instances of NP-hard problems that arise in practice may be very difficult to solve on conventional computers. There is a long history of attempts to find alternatives to current von-Neumann-computer-based methods for solving such problems, including using neural networks realized with analog electronic circuits (*1*, *2*) and using molecular computing (*3*–*5*). Both lines of investigation continue to inspire related work (*6*, *7*). A major topic of contemporary interest is the study of adiabatic quantum computation (AQC) (*8*) and quantum annealing (QA) (*9*, *10*). Sophisticated AQC/QA devices are already under study (*11*–*14*), but providing dense connectivity between qubits remains a major challenge (*15*) with important implications for the efficiency of AQC/QA systems (*16*).

Networks of coupled optical parametric oscillators (OPOs) are an alternative physical system, with an unconventional operating mechanism (*17*–*20*), for solving the Ising problem (*21*, *22*), and by extension many other combinatorial optimization problems (*23*). Formally, the $N$-spin Ising problem is to find the configuration of spins $\sigma_i \in \{-1,+1\}$ ($i$ = 1, ..., $N$) that minimizes the energy function $H = -\sum_{1\le i<j\le N} J_{ij}\sigma_i\sigma_j \sum_{1\le i\le N} h_i\sigma_i$, where the particular problem instance being solved is specified by the $N \times N$ matrix $J$ (with elements $J_{ij}$) and the length-$N$ vector $h$ (with elements $h_i$).

We have realized a system with a scalable architecture that uses measurement-feedback in place of a network of optical delay lines (which were used in initial, low-connectivity, non-reprogrammable demonstrations of the concept (*18*, *24*, *25*)). Our 100-spin Ising machine allows connections between any spin and any other spin, and is fully programmable. We show that measurement-feedback-based OPO Ising machines can solve many different Ising problems, and in cases where exact solutions are not easy to obtain, we can find good approximate solutions.

The schematic of our experimental setup (Fig. 1) shows that our Ising machine is formed by the combination of time-division-multiplexed OPOs (*18*) in a single fiber-ring cavity, with measurement and feedback (injection) stages that act to couple the pulses in the cavity such that the Ising Hamiltonian is realized. Details are provided in the Supplementary Materials (*26*).

We have focused our experiments on Ising problems on undirected, unweighted graphs ($V$ (vertices), $E$ (edges)), where $J_{ij}$ = –1 when Spin $i$ and Spin $j$ are connected, and $J_{ij}$ = 0 otherwise, and for which the linear (Zeeman) terms $h_i$ are zero. An Ising problem of this form is equivalent to the MAX-CUT problem on the underlying graph (*17*). MAX-CUT is the problem of partitioning the vertices of a graph into two disjoint subsets such that the number of edges between the two subsets is maximized; the partition is called a cut. MAX-CUT remains NP-hard even when the input is restricted to unweighted cubic graphs (*27*). We refer interchangeably to the MAX-CUT problem and to the Ising problem, and the solutions thereof. The energy of a particular spin configuration $\{\sigma_i\}_{i=1,...,N}$ for an Ising problem is given by

$H(\{\sigma_i\}) = -\sum_{1\le i<j\le N} J_{ij}\sigma_i\sigma_j - \sum_{1\le i\le N} h_i\sigma_i$ . The same spin configuration $\{\sigma_i\}$ represents a cut of size $C(\{\sigma_i\}) = -\frac{1}{2}\sum_{1\le i<j\le N} J_{ij} - \frac{1}{2}H(\{\sigma_i\})$; i.e., there is a direct mapping between the energies in the Ising problem and the cut sizes in the MAX-CUT problem, and we note that minimizing the Ising energy maximizes the cut.

Figure 2A shows the unweighted, undirected Möbius Ladder (cubic) graph with $N$ = 16 vertices. We programmed the corresponding $J$ matrix into our feedback electronics, and ran the problem on our experimental apparatus. Figure 2B shows, from a single run of this single problem instance, the evolution of the in-phase component of each OPO pulse ($c_i$) as a function of the number of times each pulse circulated around the cavity (the number of roundtrips). The computation time is given by $T_{comp} = T_{rt}N_{rt}$, where $T_{rt}$ = 1.6 μs is the single roundtrip time and $N_{rt}$ is the number of roundtrips. Each spin $\sigma_i$ in the Ising problem is represented by a single OPO pulse; if the in-phase component $c_i$ of the $i$th OPO pulse is less than zero, i.e., $c_i$ < 0, we make the spin assignment $\sigma_i$ = −1, and if the in-phase component is greater than zero, i.e., $c_i$ > 0, we make the spin assignment $\sigma_i$ = +1. As the feedback signal level is gradually increased, the OPO amplitudes increase. Most of the OPOs obtain their ultimate signs by Roundtrip 60. By Roundtrip 100, all the OPOs have reached a steady state. Figure 2C shows the graph cut size, or equivalently the Ising energy, represented by the spin configuration after each roundtrip for the run shown in Fig. 2B. We see that the system evolves toward solutions representing larger graph cuts, or equivalently lower Ising energies, and the steady-state configuration is that of a ground state. The system finds the ground state within 120 μs. If we rerun the computation many times, we find that our system always returns the optimal solution for this particular problem instance (Fig. 2D). Figure 2, E and F, shows the distributions of obtained solutions for two other $N$ = 16 cubic graphs. In both cases the system finds the ground state in a large fraction of the runs, and when the system does not return a ground state, it returns a state that has energy close to that of the ground state, i.e., a good approximate solution. To illustrate that these instances are not special cases for which the Ising machine finds exact solutions (ground states), we attempted to solve all possible problem instances of $N$ = 16 cubic graphs, of which there are 4060. Figure 2G shows that we were able to find ground states with probability greater than 20% for every single instance. In this experiment, and all that follow, every run was set to proceed for $N_{rt}$ = 300 roundtrips, i.e., a computation time of $T_{comp}$ = 480 μs.

We next explored how the Ising machine performs as a function of the size of the problem. In this first scaling study, we used the Möbius Ladder graphs with varying size. This is a convenient choice as there is a closed-form solution for the maximum cut and Ising energy for every instance in this family of graphs. The Möbius Ladder graphs with $N$ = 8, 12, ..., 100 were solved (Fig. 3A). For each instance we performed multiple sets of 100 runs. Each 100-run set resulted in a solution-energy histogram (Fig. 3B shows an example for $N$ = 8). Note that for the runs in which the ground state is not found, the system again finds good approximate solutions (Fig. 3, C and D).

To understand how the performance of our system scales as a function of problem size for more general problems, 10 random instances of cubic graphs were generated for each graph size $N$ = 10, 20, ..., 100, and each instance run on our apparatus. Figure 4A shows the success probabilities for each instance, aggregated by graph size. In contrast to the previous results, not only the probability of obtaining a ground state, but also the probability of obtaining a solution that is within $x$% of the optimal (maximum cut) solution is shown. The error bars indicate a spread in success probabilities primarily due to the fact that different random instances of each size may be more or less difficult to solve.

Figure 4B shows, for each graph size, the total computation time required to obtain a solution with the given accuracy with probability 99% within that time, and is derived directly from Fig. 4A. The total time is given by $T_{comp} \times \log(1 - 0.99)/\log(1 - ps)$, where $ps$ is the corresponding success probability from Fig. 4A. The total computation time required to obtain ground states (100% accuracy) grows rapidly with problem size $N$, although it is still small in absolute terms for $N$ = 100: less than 200 ms. The growth in total computation time is far less severe when the required solution accuracy is reduced: for 95% accuracy, the required time increases from approximately 1 ms when $N$ = 10 to approximately 4 ms when $N$ = 100; for 90% accuracy, the required time remains roughly constant at approximately 1 ms.

Figure 4, C and D, shows the OPO amplitudes and cut sizes/energies, respectively, as a function of the number of roundtrips for a single run on a single non-regular random graph instance with $N$ = 100 vertices and $|E| = 495$ edges. We see that the global optimum is reached within 100 μs, and the system reaches a steady state after approximately 120 μs. This graph instance is one of 10 instances that were generated having 495 edges. We generated 10 random graphs with a fixed number of edges, for each of $|E| = 50, 495, 990, 1485, 1980, 2475, 2970, 3465, 3960, 4455, 4900$, and ran these instances on our apparatus. Figure 4E shows the results of this study of the performance on random

graphs as a function of edge density $d = 2|E|/\left[|V|\left(|V|-1\right)\right]$; the system was able to find good solutions for all the attempted densities.

OPO Ising machines have the potential to harness a number of quantum features, including squeezing and superposition (*20*). Pulsed OPOs already have a substantial quantum-mechanical nature (*28*), and networks of OPOs can generate spatial multimode entanglement (*19*). The experimental system reported in this work is well-described by a quantum-mechanical model (*20*) (with very good agreement between our experimental results and numerical simulation results (*26*)). However, the extent to which classical models can capture the behavior of OPO Ising machines is not yet known, and follow-up studies are needed to determine the fundamental computational power of OPO Ising machines. Two future modifications to the experiment that could increase the relevance of quantum mechanics are reducing the cavity round-trip loss, and injecting squeezed vacuum states into the open port of the measurement beamsplitter (*29*), which is predicted to improve the success probability (*26*).

While we find the overall direction of OPO Ising machines promising, the techniques we have demonstrated are not necessarily restricted to OPO Ising machines, and photonic-AQC and boson-sampling (*30*) experiments, amongst others, may be able to adapt our methods.

## REFERENCES AND NOTES


1. J. J. Hopfield, D. W. Tank, Computing with neural circuits: A model. *Science* **233**, 625–633 (1986). Medline doi:10.1126/science.3755256
2. D. Tank, J. Hopfield, Simple 'neural' optimization networks: An A/D converter, signal decision circuit, and a linear programming circuit. *IEEE Trans. Circ. Syst.* **33**, 533–541 (1986). doi:10.1109/TCS.1986.1085953
3. L. M. Adleman, Molecular computation of solutions to combinatorial problems. *Science* **266**, 1021–1024 (1994). Medline doi:10.1126/science.7973651
4. R. J. Lipton, DNA solution of hard computational problems. *Science* **268**, 542–545 (1995). Medline doi:10.1126/science.7725098
5. R. S. Braich, N. Chelyapov, C. Johnson, P. W. K. Rothemund, L. Adleman, Solution of a 20-variable 3-SAT problem on a DNA computer. *Science* **296**, 499–502 (2002). Medline doi:10.1126/science.1069528
6. M. Ercsey-Ravasz, Z. Toroczkai, Optimization hardness as transient chaos in an analog approach to constraint satisfaction. *Nat. Phys.* **7**, 966–970 (2011). doi:10.1038/nphys2105
7. L. Qian, E. Winfree, J. Bruck, Neural network computation with DNA strand displacement cascades. *Nature* **475**, 368–372 (2011). Medline doi:10.1038/nature10262
8. E. Farhi, J. Goldstone, S. Gutmann, J. Lapan, A. Lundgren, D. Preda, A quantum adiabatic evolution algorithm applied to random instances of an NP-complete problem. *Science* **292**, 472–475 (2001). Medline doi:10.1126/science.1057726
9. T. Kadowaki, H. Nishimori, Quantum annealing in the transverse Ising model. *Phys. Rev. E Stat. Phys. Plasmas Fluids Relat. Interdiscip. Topics* **58**, 5355–5363 (1998). doi:10.1103/PhysRevE.58.5355
10. J. Brooke, D. Bitko, T. F. Rosenbaum, G. Aeppli, Quantum annealing of a disordered magnet. *Science* **284**, 779–781 (1999). Medline doi:10.1126/science.284.5415.779
11. M. W. Johnson, M. H. Amin, S. Gildert, T. Lanting, F. Hamze, N. Dickson, R. Harris, A. J. Berkley, J. Johansson, P. Bunyk, E. M. Chapple, C. Enderud, J. P. Hilton, K. Karimi, E. Ladizinsky, N. Ladizinsky, T. Oh, I. Perminov, C. Rich, M. C. Thom, E. Tolkacheva, C. J. Truncik, S. Uchaikin, J. Wang, B. Wilson, G. Rose, Quantum annealing with manufactured spins. *Nature* **473**, 194–198 (2011). Medline doi:10.1038/nature10012
12. T. F. Rønnow, Z. Wang, J. Job, S. Boixo, S. V. Isakov, D. Wecker, J. M. Martinis, D. A. Lidar, M. Troyer, Defining and detecting quantum speedup. *Science* **345**, 420–424 (2014). Medline doi:10.1126/science.1252319
13. S. Boixo, T. F. Rønnow, S. V. Isakov, Z. Wang, D. Wecker, D. A. Lidar, J. M. Martinis, M. Troyer, Evidence for quantum annealing with more than one hundred qubits. *Nat. Phys.* **10**, 218–224 (2014). doi:10.1038/nphys2900
14. R. Barends, A. Shabani, L. Lamata, J. Kelly, A. Mezzacapo, U. Las Heras, R. Babbush, A. G. Fowler, B. Campbell, Y. Chen, Z. Chen, B. Chiaro, A. Dunsworth, E. Jeffrey, E. Lucero, A. Megrant, J. Y. Mutus, M. Neeley, C. Neill, P. J. O'Malley, C. Quintana, P. Roushan, D. Sank, A. Vainsencher, J. Wenner, T. C. White, E. Solano, H. Neven, J. M. Martinis, Digitized adiabatic quantum computing with a superconducting circuit. *Nature* **534**, 222–226 (2016). Medline doi:10.1038/nature17658
15. P. I. Bunyk, E. M. Hoskinson, M. W. Johnson, E. Tolkacheva, F. Altomare, A. J. Berkley, R. Harris, J. P. Hilton, T. Lanting, A. J. Przybysz, J. Whittaker, Architectural Considerations in the Design of a Superconducting Quantum Annealing Processor. *IEEE Trans. Appl. Supercond.* **24**, 1–10 (2014). doi:10.1109/TASC.2014.2318294
16. E. G. Rieffel, D. Venturelli, B. O'Gorman, M. B. Do, E. M. Prystay, V. N. Smelyanskiy, A case study in programming a quantum annealer for hard operational planning problems. *Quant. Inform. Process.* **14**, 1–36 (2014). doi:10.1007/s11128-014-0892-x
17. Z. Wang, A. Marandi, K. Wen, R. L. Byer, Y. Yamamoto, Coherent Ising machine based on degenerate optical parametric oscillators. *Phys. Rev. A* **88**, 063853 (2013). doi:10.1103/PhysRevA.88.063853
18. A. Marandi, Z. Wang, K. Takata, R. L. Byer, Y. Yamamoto, Network of time-multiplexed optical parametric oscillators as a coherent Ising machine. *Nat. Photonics* **8**, 937–942 (2014). doi:10.1038/nphoton.2014.249
19. K. Takata, A. Marandi, Y. Yamamoto, Quantum correlation in degenerate optical parametric oscillators with mutual injections. *Phys. Rev. A* **92**, 043821 (2015). doi:10.1103/PhysRevA.92.043821
20. Y. Haribara, S. Utsunomiya, Y. Yamamoto, Computational Principle and Performance Evaluation of Coherent Ising Machine Based on Degenerate Optical Parametric Oscillator Network. *Entropy* **18**, 151 (2016). doi:10.3390/e18040151
21. F. Barahona, On the computational complexity of Ising spin glass models. *J. Phys. Math. Gen.* **15**, 3241–3253 (1982). doi:10.1088/0305-4470/15/10/028
22. S. Istrail, *Proceedings of the Thirty-second Annual ACM Symposium on Theory of Computing*, STOC (2000), pp. 87–96.
23. A. Lucas, Ising formulations of many NP problems. *Front. Phys.* **2**, 5 (2014). doi:10.3389/fphy.2014.00005
24. K. Takata *et al.*, *Sci. Rep.* **6**, 340897 (2016).
25. T. Inagaki, K. Inaba, R. Hamerly, K. Inoue, Y. Yamamoto, H. Takesue, Large-scale Ising spin network based on degenerate optical parametric oscillators. *Nat. Photonics* **10**, 415–419 (2016). doi:10.1038/nphoton.2016.68
26. Materials and methods are available as supplementary materials on *Science* Online.
27. M. R. Garey, D. S. Johnson, L. Stockmeyer, Some simplified NP-complete graph problems. *Theor. Comput. Sci.* **1**, 237–267 (1976). doi:10.1016/0304-3975(76)90059-1
28. J. Roslund, R. M. de Araújo, S. Jiang, C. Fabre, N. Treps, Wavelength-multiplexed quantum networks with ultrafast frequency combs. *Nat. Photonics* **8**, 109 (2014). doi:10.1038/nphoton.2013.340
29. W. J. Munro, M. D. Reid, Transient macroscopic quantum superposition states in degenerate parametric oscillation using squeezed reservoir fields. *Phys. Rev. A* **52**, 2388 (1995). doi:10.1103/PhysRevA.52.2388
30. K. R. Motes, A. Gilchrist, J. P. Dowling, P. P. Rohde, Scalable boson sampling with time-bin encoding using a loop-based architecture. *Phys. Rev. Lett.* **113**, 120501 (2014). Medline doi:10.1103/PhysRevLett.113.120501
31. M. Denil, N. de Freitas, *NIPS Deep Learning and Unsupervised Feature Learning Workshop* (2011).

32. V. Dumoulin, I. J. Goodfellow, A. Courville, Y. Bengio, *arXiv:1312.5258* (2013).
33. F. Rendl, G. Rinaldi, A. Wiegele, Solving Max-Cut to optimality by intersecting semidefinite and polyhedral relaxations. *Math. Program.* **121**, 307–335 (2008). doi:10.1007/s10107-008-0235-8
34. U. Benlic, J.-K. Hao, Breakout Local Search for the Max-Cutproblem. *Eng. Appl. Artif. Intell.* **26**, 1162–1173 (2013). doi:10.1016/j.engappai.2012.09.001
35. S. W. Shin, G. Smith, J. A. Smolin, U. Vazirani, *arXiv:1401.7087* (2014).
36. A. Perdomo-Ortiz, N. Dickson, M. Drew-Brook, G. Rose, A. Aspuru-Guzik, Finding low-energy conformations of lattice protein models by quantum annealing. *Sci. Rep.* **2**, 571 (2012). Medline doi:10.1038/srep00571
37. C. C. McGeoch, C. Wang, *Proceedings of the ACM International Conference on Computing Frontiers*, CF '13 (ACM, New York, NY, USA, 2013), pp. 23:1–23:11.
38. D. Venturelli *et al.*, *Phys. Rev. X* **5**, 031040 (2015).
39. D. Venturelli, D. J. J. Marchand, G. Rojo, *arXiv:1506.08479* (2015).
40. V. S. Denchev *et al.*, *arXiv:1512.02206* (2015).
41. Z. Bian *et al.*, *arXiv:1603.03111* (2016).
42. S. Mandra, Z. Zhu, W. Wang, A. Perdomo-Ortiz, H. G. Katzgraber, *arXiv:1604.01746* (2016).
43. D. Maruo, S. Utsunomiya, Y. Yamamoto, Truncated Wigner theory of coherent Ising machines based on degenerate optical parametric oscillator network. *Phys. Scr.* **91**, 083010 (2016). doi:10.1088/0031-8949/91/8/083010
44. R. Hamerly *et al.*, *arXiv:1605.08121* (2016).
45. D. F. Walls, G. J. Milburn, *Quantum Optics* (Springer-Verlag, Berlin, 2008), second edn.
46. D. T. Pegg, S. M. Barnett, *J. Mod. Opt.* **44**, 225 (1997).
47. P. Alimonti, V. Kann, *Algorithms and Complexity*, G. Bongiovanni, D. P. Bovet, G. D. Battista, eds., no. 1203 in Lecture Notes in Computer Science (Springer Berlin Heidelberg, 1997), pp. 288–298. DOI: 10.1007/3-540-62592-5_80.
48. J. Sima, S. E. Schaeffer, *arXiv:cs/0506100* (2005).
49. B. Bollobás, A Probabilistic Proof of an Asymptotic Formula for the Number of Labelled Regular Graphs. *Eur. J. Combin.* **1**, 311–316 (1980). doi:10.1016/S0195-6698(80)80030-8
50. N. C. Wormald, *Surveys in combinatorics*, J. D. Lamb, D. A. Preece, eds., London Math. Soc. Lecture Note Series (Canterbury, 1999), pp. 239–298.
51. G. Bounova, Topological evolution of networks: case studies in the US airlines and language Wikipedias, Ph.D. Thesis, Massachusetts Institute of Technology (2009).
52. M. Yamaoka *et al.*, *2015 IEEE International Solid-State Circuits Conference (ISSCC)* (2015), pp. 1–3.
53. Y. Okawachi, M. Yu, K. Luke, D. O. Carvalho, S. Ramelow, A. Farsi, M. Lipson, A. L. Gaeta, Dual-pumped degenerate Kerr oscillator in a silicon nitride microresonator. *Opt. Lett.* **40**, 5267–5270 (2015). Medline doi:10.1364/OL.40.005267
54. P. C. Humphreys, B. J. Metcalf, J. B. Spring, M. Moore, X. M. Jin, M. Barbieri, W. S. Kolthammer, I. A. Walmsley, Linear optical quantum computing in a single spatial mode. *Phys. Rev. Lett.* **111**, 150501 (2013). Medline doi:10.1103/PhysRevLett.111.150501
55. S. Aaronson, A. Arkhipov, *Proceedings of the Forty-third Annual ACM Symposium on Theory of Computing*, STOC '11 (ACM, New York, NY, USA, 2011), pp. 333–342.
56. Y. He *et al.*, *arXiv:1603.04127* (2016).
57. J. Huh, G. G. Guerreschi, B. Peropadre, J. R. McClean, A. Aspuru-Guzik, Boson sampling for molecular vibronic spectra. *Nat. Photonics* **9**, 615–620 (2015). doi:10.1038/nphoton.2015.153
58. U. L. Andersen, T. Gehring, C. Marquardt, G. Leuchs, 30 years of squeezed light generation. *Phys. Scr.* **91**, 053001 (2016). doi:10.1088/0031-8949/91/5/053001

## ACKNOWLEDGMENTS

This research was funded by the Impulsing Paradigm Change through Disruptive Technologies (ImPACT) Program of the Council of Science, Technology and Innovation (Cabinet Office, Government of Japan). PLM was partially supported by a Stanford Nano- and Quantum Science and Engineering Postdoctoral Fellowship. We thank Ken Leedle, Andrew Ceballos, Kai Wen and Zhe Wang for technical assistance, and Michel Digonnet, Brian Lantz, Tatsuhiro Onodera, Edwin Ng, Timothee Leleu, Charles Limouse, Dodd Gray, Gil Tabak and Nikolas Tezak for helpful discussions.

## SUPPLEMENTARY MATERIALS

www.sciencemag.org/cgi/content/full/science.aah5178/DC1
Materials and Methods
Supplementary Text
Figs. S1 to S5
References (*31–58*)

8 July 2016; accepted 26 September 2016
Published online 20 October 2016
10.1126/science.aah5178

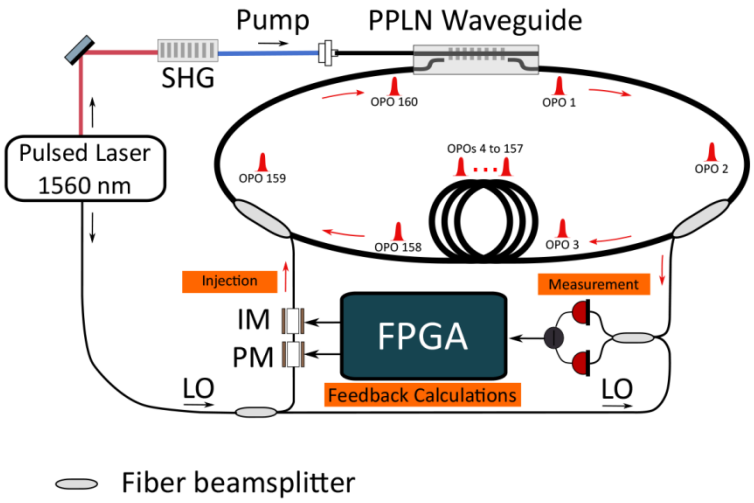


**Fig. 1. Experimental schematic of a measurement-feedback-based coherent Ising machine.** A time-division-multiplexed pulsed degenerate optical parametric oscillator is formed by a nonlinear crystal (PPLN) in a fiber ring cavity containing 160 pulses. A fraction of each pulse is measured and used to compute a feedback signal that effectively couples the otherwise-independent pulses in the cavity. IM: intensity modulator; PM: phase modulator; LO: local oscillator; SHG: second-harmonic generation; FPGA: field-programmable gate array.

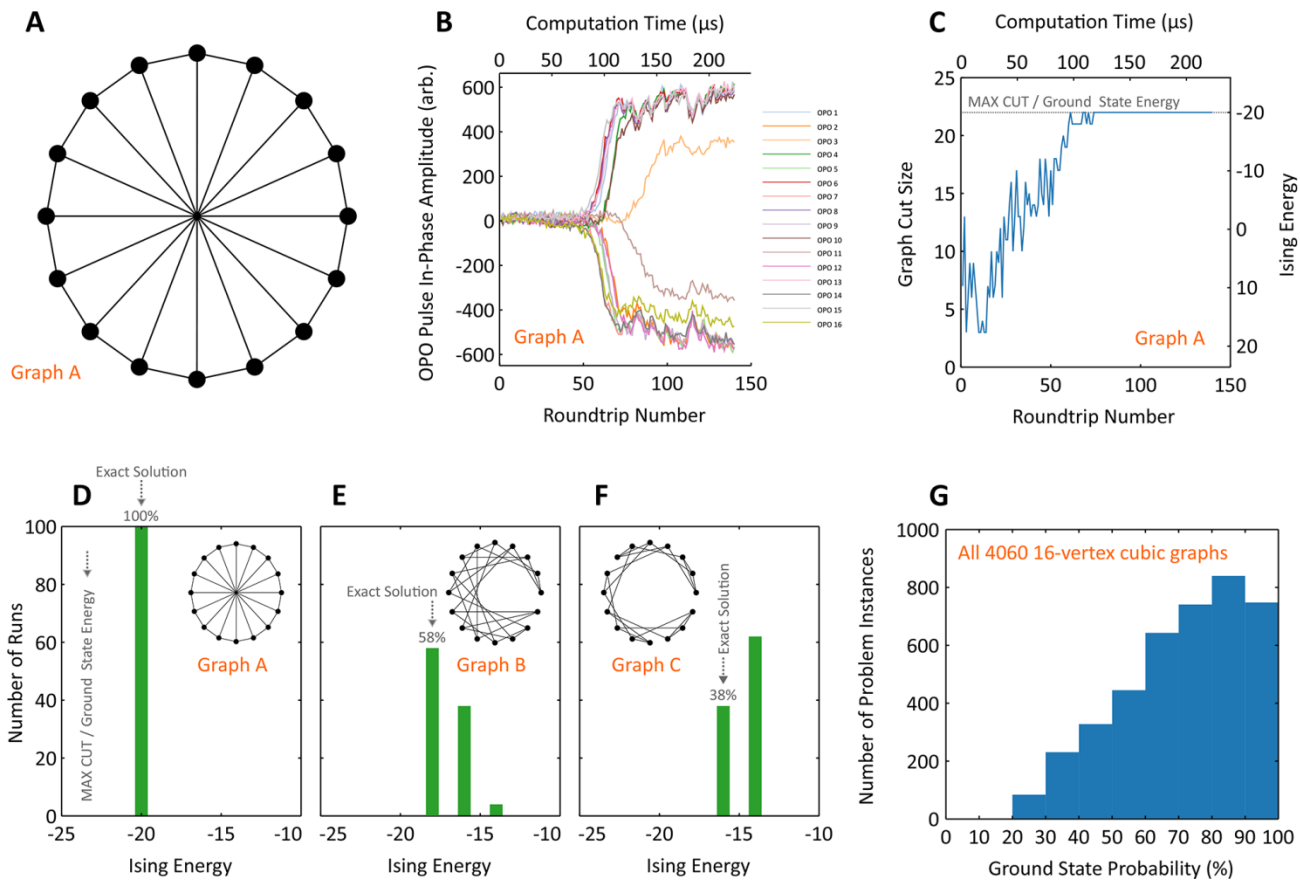


**Fig. 2. Results with $N = 16$ cubic graphs.** (**A**) A Möbius Ladder graph with $N = 16$ vertices. (**B**) The evolution of the in-phase components $c_i$ of the $N = 16$ OPO pulses as a function of the computation time. (**C**) The graph cut size achieved as a function of the computation time. (**D** to **F**) Histograms of obtained solutions in 100 runs for the graphs shown in the insets. (**G**) Histogram of the observed probabilities of obtaining a ground state in a single run, for all 4060 unweighted, undirected cubic graphs with $N = 16$ vertices.

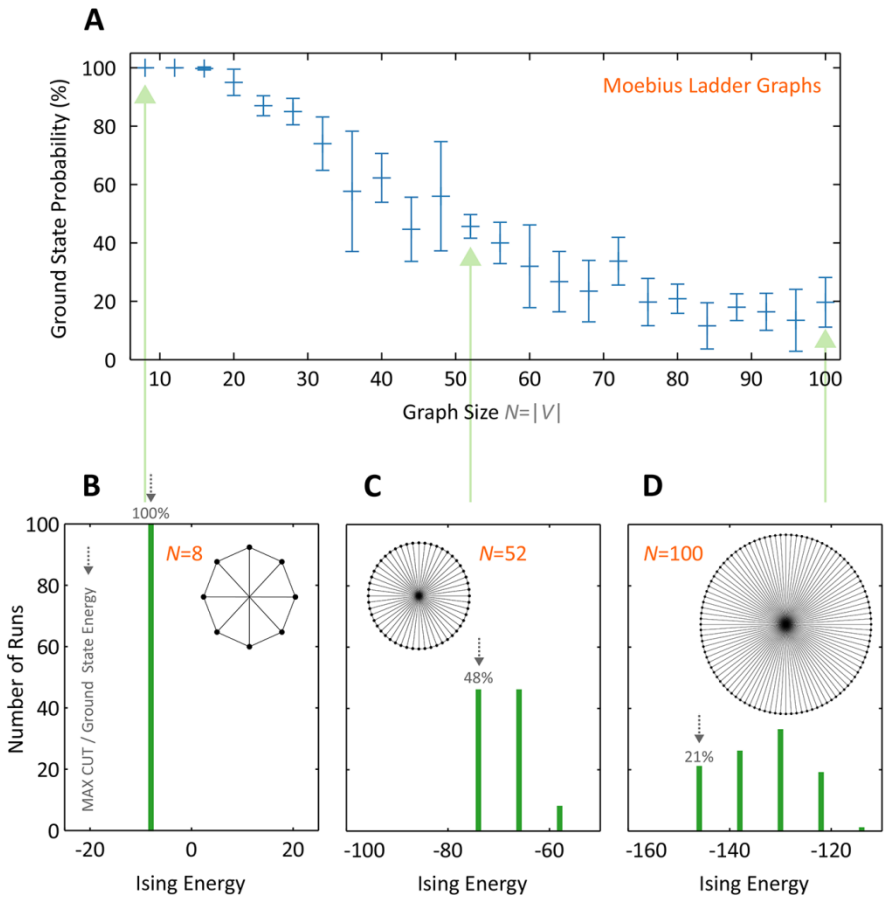


**Fig. 3. Results with various-size Möbius Ladder graphs.** (**A**) Observed probability of obtaining a ground state of the Möbius Ladder graph in a single run, as a function of the size *N* of the graph. Multiple 100-run batches were performed for each graph size to obtain the standard deviations, which are shown as error bars. (**B** to **D**) Histograms of obtained solutions in 100 runs for the graphs shown in the insets.

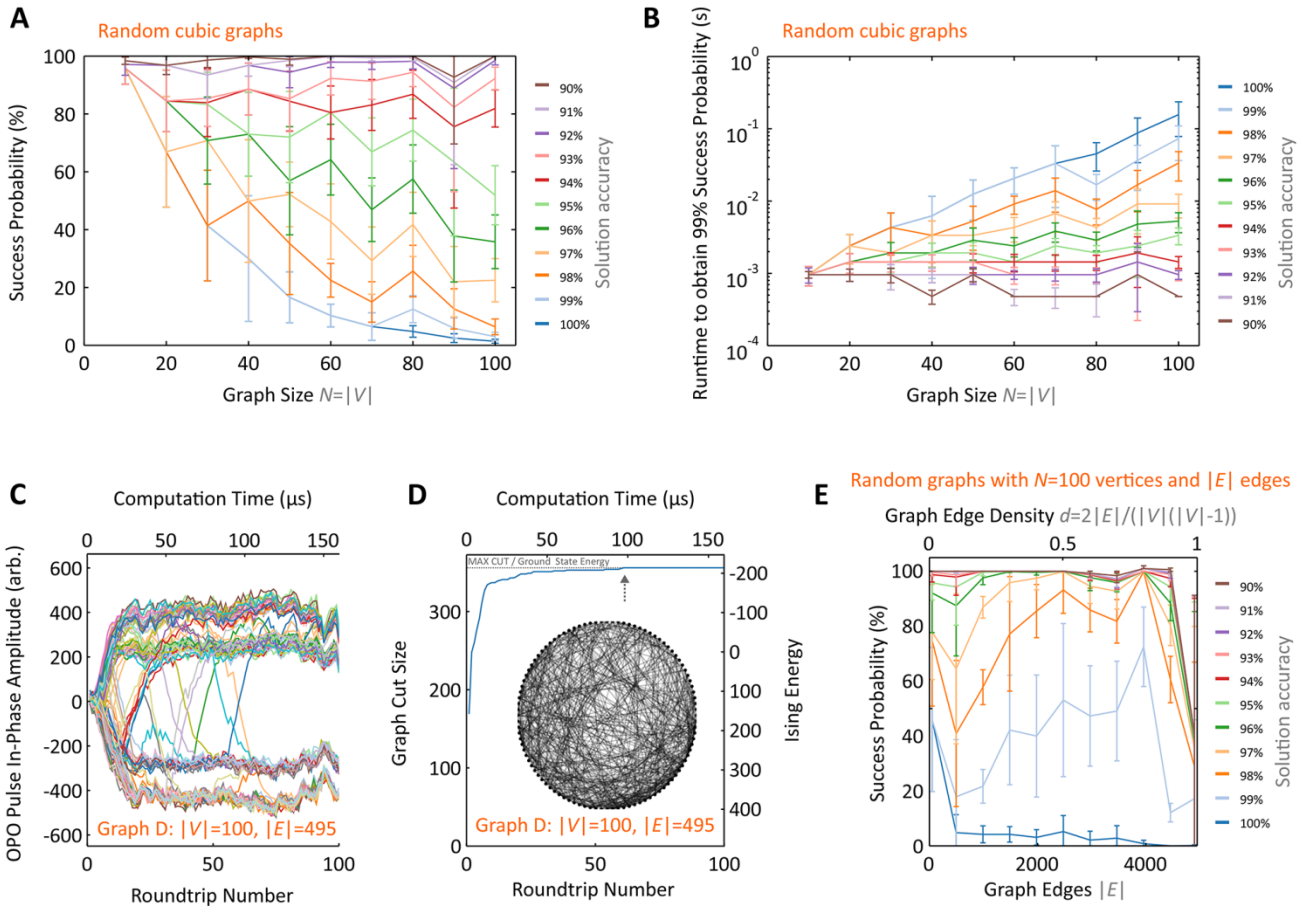


**Fig. 4. Results with various-size and various-density random graphs.** (**A**) Observed probability of obtaining a solution whose cut size is at least *x*% of the global optimum (maximum cut), as a function of graph size *N*, for random cubic graph instances. Error bars indicate one standard deviation, which is dominated by the difference in difficulty between the various problem instances. (**B**) The runtime that would be required to obtain a solution of a particular accuracy with 99% probability. (**C**) The evolution of the in-phase components $c_i$ of the $N = 100$ OPO pulses as a function of the computation time, for a single run with the graph shown in the inset of Panel D. (**D**) The graph cut size achieved as a function of the computation time. Inset: the graph being solved. (**E**) Observed success probability of obtaining a solution with a particular accuracy as a function of the density of edges in the graph. Experiments were performed on randomly-generated $N = 100$-vertex graphs with fixed numbers of edges. Error bars indicate one standard deviation.





**A fully-programmable 100-spin coherent Ising machine with all-to-all connections**

Peter L. McMahon, Alireza Marandi, Yoshitaka Haribara, Ryan Hamerly, Carsten Langrock, Shuhei Tamate, Takahiro Inagaki, Hiroki Takesue, Shoko Utsunomiya, Kazuyuki Aihara, Robert L. Byer, M. M. Fejer, Hideo Mabuchi and Yoshihisa Yamamoto (October 20, 2016)
published online October 20, 2016

Editor's Summary



*Science* (print ISSN 0036-8075; online ISSN 1095-9203) is published weekly, except the last week in December, by the American Association for the Advancement of Science, 1200 New York Avenue NW, Washington, DC 20005. 